Evaluation of Aluminum-Lithium Alloys in Compression-Stiffened Aircraft Structures

J. C. Ekvall* and D. J. Chellman†
Lockheed Aeronautical Systems Company, Burbank, California

Aluminum-lithium (Al-Li) alloys represent an area of considerable interest to the aircraft industry because of the potential for high structural efficiencies compared to conventional alloy products. The reported work addresses the identification and characterization of a candidate Al-Li alloy that demonstrates promise for use in 7075 aluminum structural applications. Heat treatment studies were conducted initially to select a suitable combination of strength, ductility, and toughness. Mechanical property evaluations comprising static and cyclic testing were subsequently performed on extruded bar materials, and compared to baseline 7075 aluminum extrusions. The structural behavior was established by compression testing of stiffened panels, typical of those used in airframe construction. Experimental findings and predictions are discussed in terms of the properties of materials. A structural weight savings of between 8 and 13% was shown for Al-Li alloy materials in compression critical components.

Nomenclature

c	= end fixity coefficient
da/dN	= fatigue crack growth rate, in./cycle
DADT	= durability and damage tolerance
e	= tensile elongation, percent in four-dimensional
E_c	= compression modulus of elasticity, psi
E_s	= secant modulus of elasticity, psi
E_t	= tension or tangent modulus of elasticity, psi
F_{cr}	= critical buckling stress, ksi
F_{cy}	= compression yield stress, ksi
F_{max}	= maximum net area stress, ksi
F_{su}	= ultimate shear stress, ksi
F_{tu}	= ultimate tensile stress, ksi
F_{ty}	= 0.2% offset tensile yield stress, ksi
$F_{0.7}$	= secant yield stress at $0.7E$, ksi
f	= flange width, in.
k_c	= compression buckling coefficient
K_{Ic}	= plane strain fracture toughness, ksi-in.$^{1/2}$
K_Q	= conditional plane strain fracture toughness, ksi-in.$^{1/2}$
L	= longitudinal grain direction
LT	= long-transverse grain direction
l	= total column length, in.
NTS	= notched tensile stress, ksi
n	= Ramberg-Osgood shape factor
RA	= reduction in area, %
t	= flange thickness, in.
$-$T3X	= naturally aged heat treatment temper
$-$T8X	= artificially aged heat treatment temper
ρ	= radius of gyration, in.

Introduction

THE family of Al-Li alloys offers the potential for significant weight savings in aircraft structures due to density reductions and stiffness improvements. The newly emerging Al-Li alloys have been designed as functional replacements for various mill products based on conventional 7075 and 2024 aluminum alloys. Specific mechanical and physical property targets have been established by the major aluminum producers for these first generation Al-Li alloy products.[1-3] Typically, the development goals represent equivalent properties to the incumbent aluminum alloys, but with alloy density reductions of 7–10% and elastic modulus improvements of 10–15%.

The accelerated development of low-density Al-Li alloys stems from weight savings analyses and parametric design studies performed by various aerospace companies in the 1978–1986 time frame.[4-6] The relationship between weight savings and property improvements for a generic fighter airframe from one such study is illustrated in Fig. 1. These findings generally show that a reduction in alloy density is more effective in improving performance and payload than commensurate improvements in any other single primary property such as strength or modulus, or second-tier properties such as toughness or fatigue. Over the same period of time, several major aluminum producers in the U.S., England, and France started developing an advanced ingot casting technology for Li-containing aluminum alloys. Screening evaluations have been conducted on a wide range of Al-Li alloy compositions to identify the most suitable candidates for satisfying the property targets. A number of Al-Li alloys have been registered and produced in limited quantities for evaluation purposes. The community of aluminum producers and aerospace users are now actively pursuing the maturation of low-density Al-Li alloy materials for applications in aircraft structures.

Alloying and processing development activities are currently underway at the major aluminum suppliers to support the anticipated need for Al-Li alloy products. A number of alloys, heat treatment tempers, and product forms have been introduced and scheduled for delivery to the aircraft industry. However, to date, only limited quantities of materials have been available for property evaluations. Complex issues involving molten metal treatment and fabrication schedules apparently have slowed the emergence of suitable evaluation materials. In recognition of this situation, LASC-Burbank in cooperation with Naval Surface Weapons Center (NSWC) initiated a series of development studies to identify promising Al-Li alloy systems for structural applications.[7] One such candidate alloy, suitable for replacing 7075-TXX aluminum extrusions, was cast and fabricated into the two wrought product forms shown in Fig. 2. Some of the material proper-

Presented as Paper 87-0785-CP at the AIAA/ASME/AHS/ASEE 28th Structures, Structural Dynamics and Materials Conference, Monterey, CA, April 6–8, 1987; received May 13, 1987; revision received May 2, 1988.

*Research and Development Engineer. Member AIAA.
†Senior Research Specialist. Member AIAA.

ties and structural testing conducted on this Al-Li alloy are described in Ref. 8 and in this paper.

Materials Development

LASC-Burbank has been actively involved in the development and evaluation of Al-Li alloy materials since 1978. Diversified efforts from alloy optimization to process development have been undertaken to promote the acceptance of these low-density aluminum alloys as aircraft structural materials. Recent laboratory scale studies in cooperation with NSWC have led to the identification of several candidate alloy systems that represent replacements for conventional 7075-T6X, 7075-T76, 7075-T73X, and 2024-T3X aluminum alloys.[9,10] In the present evaluation effort, an Al-Li alloy exhibiting strength and damage tolerant properties competitive with 7075 aluminum is described in terms of mechanical properties and structural behavior. Integrally stiffened compression panels typically encountered in airframe construction have been designed and tested to verify the structural efficiency of the candidate Al-Li alloy.

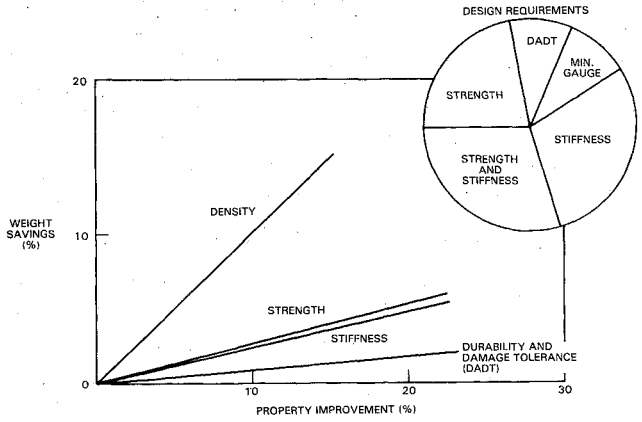

Fig. 1 Weight savings potential as a function of property improvement for advanced fighter aircraft.

Materials Fabrication

A quaternary Al-Li-Cu-Mg-(Zr) alloy composition was selected for further development at LASC-Burbank based on a series of screening evaluations on laboratory size billets. The nominal chemistry limits established for the optimized Al-Li alloy, designated LOCKALITE, are given in Table 1. A 1000 lb, 12 in. diam by 106 in. long ingot was cast of the LOCKALITE composition at International Light Metals, Inc. (formerly Martin-Marietta Aluminum) in Torrance, California. Chemical analyses indicated that the target composition was achieved within ± 0.10 weight percent. The cast billet was scalped to 10.5 in. diam to remove oxide scale and porosity at the ends of the casting. A homogenization treatment of 975°F for 12 h was used to minimize solute segregation prior to final wrought product fabrication. Several product forms were subsequently processed from the LOCKALITE ingot, including the two extruded shapes shown in Fig. 2. The extrusion products represent the first Al-Li shaped extrusions available to Lockheed for test and evaluation. The wing plank section was selected to establish the workability of complex shapes used typically in the aerospace industry. In general, the candidate Al-Li alloy exhibited excellent hot working characteristics, and the resultant wrought products appeared to be visually equivalent to conventional high-strength aluminum alloys.

Heat Treatment Studies

The 1 × 4 in. rectangular bar and wing plank section were directly extruded from the 10.5 in. diam extrusion charge, resulting in extrusion ratios of 22:1 and 18:1, respectively. The two extrusions were processed at a temperature of 750°F using standard conditions for high-strength aluminum alloy products. Differential scanning calorimetry (DSC) measure-

Table 1 Alloy chemistries and physical properties for candidate IM Al-Li alloy (LOCKALITE)

Product/ location	Composition (weight percent)						Density, lb/in.^{3}	Elastic modulus, × 10^6 psi
	Li	Cu	Mg	Zr	Fe	Si		
Billet								
Target	2.20	2.50	1.10	0.12	<0.30	<0.20	—	—
Actual	2.13	2.51	1.05	0.14	0.08	0.06	—	—
Rectangular extrusion								
Center	2.16	2.56	0.96	0.13	0.09	0.08	0.0932	11.76
Edge	2.23	2.48	0.95	0.14	0.12	0.07	0.0927	11.83

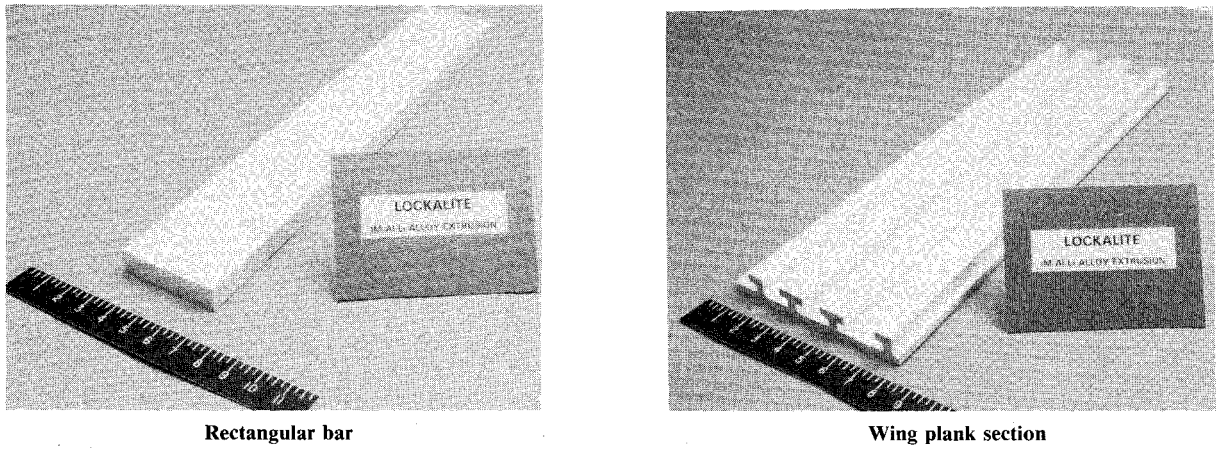

Rectangular bar Wing plank section

Fig. 2 Extruded products fabricated from IM Al-Li Alloy (LOCKALITE) billet.

ments and optical metallography examinations were conducted on the LOCKALITE alloy extrusions to determine an optimum solution treatment practice. Solution heat treatment at 990°F for 2 h was employed to ensure that all alloying elements were in complete solid solution. The extrusions were stretched a nominal 2.5–3.0% immediately following solution treatment and cold water quench, prior to any age hardening. The extruded products were supplied to LASC-Burbank in the −T3X condition for subsequent mechanical property characterization. An isothermal aging study as a function of temperature and time was conducted initially to identify candidate heat treatment tempers as shown in Table 2. Tensile tests were conducted on heat treatments that corresponded to underaged (UA), peak-aged (PA), and overaged (OA) portions of the precipitation hardening curves, in addition to the naturally aged condition (−T3X). The artificial aging temperatures under evaluation ranged from 300 to 400°F. Tensile property trends for various aging temperature and time combinations are summarized in Fig. 3. The yield and tensile strength results indicate that the age hardening peak is at-

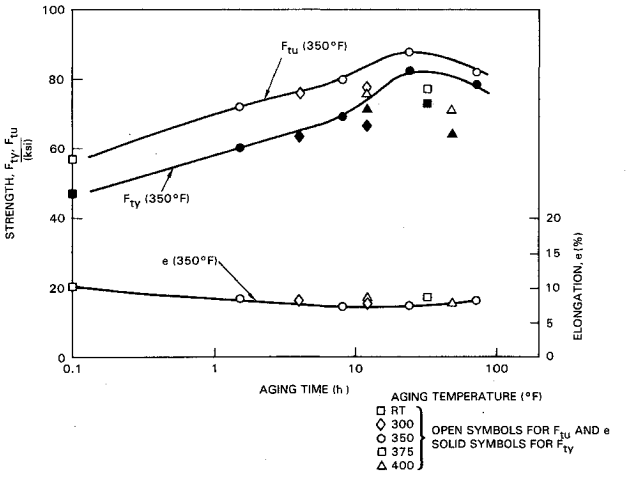

Fig. 3 Age hardening response for IM Al-Li Alloy (LOCKALITE) extrusions.

Table 2 Isothermal aging study on IM Al-Li alloy (LOCKALITE) extrusions[a]

Temper	Aging temp, °F	Aging time, h	F_{ty}, ksi	F_{tu}, ksi	e, %	RA, %	E_t, × 10^6 psi
-T3X	——	——	47.1	56.8	10.4	19.7	11.6
-T8X (UA)	300	4.0	63.4	75.8	8.2	7.6	11.5
-T8X (UA)	300	12.0	66.8	77.9	7.8	6.7	11.6
-T8X (UA)	350	1.5	60.4	72.3	8.5	6.1	11.3
-T8X (UA)	350	8.0	69.2	80.0	7.5	5.0	11.5
-T8X (PA)	350	24.0	83.2	88.3	7.6	9.4	11.7
-T8X (OA)	350	72.0	78.8	81.7	8.3	15.6	11.4
-T8X (OA)	375	32.0	73.3	77.5	8.8	17.5	11.3
-T8X (OA)	400	12.0	72.0	76.4	8.5	17.4	11.1
-T8X (OA)	400	48.0	64.1	71.4	7.8	12.4	11.2

[a]Longitudinal orientation, average of triplicate specimens.

Table 3 Mechanical property results for candidate IM Al-Li alloy (LOCKALITE) extrusion

Property	Test direction	LOCKALITE[a]	7075-T6X[b]	7075-T76[b]	7075-T73[b]
Strength					
F_{ty}, ksi	*L*	82.9	76.0	67.0	63.0
	LT	69.6	68.0	61.0	58.0
F_{tu}, ksi	L	87.1	85.0	76.0	73.0
	LT	78.6	78.0	71.0	69.0
e, %	L	8.3	7.0	7.0	8.0
	LT	6.8	7.0	7.0	8.0
E_t, × 10^6 psi	L	11.6	10.4	10.4	10.4
	LT	11.5	10.4	10.4	10.4
NTS/YS	L	1.19	1.25	——	——
	LT	1.10	1.20	——	——
F_{cy}, ksi	L	80.4	76.0	67.0	63.0
	LT	71.2	74.0	66.0	61.0
E_c, × 10^6 psi	L	11.8	10.7	10.7	10.7
	LT	11.6	10.7	10.7	10.7
F_{su}, ksi	L	42.2	44.0	41.0	39.0
	LT	42.4	40.0	——	——
Fracture toughness:					
K_Q/K_{IC}, ksi-in.$^{1/2}$	L-T	30.7	29.0	32.0	35.0
	T-L	15.6	21.0	23.0	23.0
Fatigue					
[c]F_{max}, ksi	L	23.8	26.0	22.0	21.0
[d]da/dN, × 10^{-6} in./cycle	L-T	3.2	18.0	10.0	9.0

[a]-T8X temper, aged at 350°F for 24 h.
[b]MIL-HDBK-5E design properties, "B" basis, 0.75–1.50 in. thickness.
[c]Constant amplitude fatigue, F_{max} at $N = 10^5$ cycles, $K_t = 3$, $R = +0.1$.
[d]Fatigue crack growth, da/dN at $\Delta K = 10$ ksi-in.$^{1/2}$, $R = +0.1$, $f = 20$ Hz, relative humidity > 95%.

tained for times in excess of 8 h at 350°F. Apparently the peak strength plateau is rather broad, from approximately 8 to 72 h at this intermediate temperature, with all yield strength values exceeding 75.0 ksi. Tensile property screening led to the selection of a recommended −T8X temper consisting of 350°F for 24 h.[9] For this heat treatment condition, an optimum combination of strength and ductility was obtained in the LOCKALITE alloy extrusions.

Materials Properties

The mechanical property behavior of the LOCKALITE extruded bar was determined from tests conducted using standard ASTM testing procedures. The results were obtained to facilitate comparisons with 7075-TXX aluminum extrusions and to provide a basis for interpreting the structural panel evaluations. Smooth and notched tension, compression, shear, fracture toughness, notched fatigue, and fatigue crack growth properties were established for the candidate Al-Li alloy in the recommended −T8X temper. Testing was conducted in both the *L* and *LT* grain directions. The average test results of LOCKALITE were compared with "B" basis design mechanical properties for 7075-TXX aluminum extrusions obtained from MIL-HDBK-5E in Table 3.[11]

The "B" basis properties for LOCKALITE would be 5 to 10% lower than the values given in Table 3. Therefore, the B basis properties of Al-Li would fall between the properties for 7075-T6 and 7075-T73 aluminum extrusions. Tension and compression properties are shown in Fig. 4 for the two extruded products. High strength levels in both grain orientations, ultimate of 79–87 ksi and yield of 70–83 ksi, were obtained for the LOCKALITE alloy with tensile elongations of 7 to 8%. A slightly greater tendency for anisotropic strength and modulus properties was exhibited by the Al-Li alloy extrusion. Elastic modulus improvements of 13–15% compared to 7075 aluminum were in agreement with results obtained in the aging study. Fracture toughness indications for the LOCKALITE extruded bar was determined using compact-tension (CT) fracture toughness specimens. Results of the fracture toughness tests on the Al-Li alloy are compared with several high strength aluminum alloys in Fig. 5. Due to minor differences in crack length measurements and specimen load levels, the test findings were not considered to be strictly valid K_{Ic} values. However, the K_Q toughness values appear to be equivalent to typical results for 7075-T76X and 7075-T73X aluminum extrusions. The preliminary damage tolerant and durability properties, established from notched fatigue and crack growth rate testing, met or exceeded 7075-T6X properties. For these reasons, the LOCKALITE alloy extrusion appears to be a suitable candidate for consideration in structural applications involving conventional 7075 aluminum alloy products.

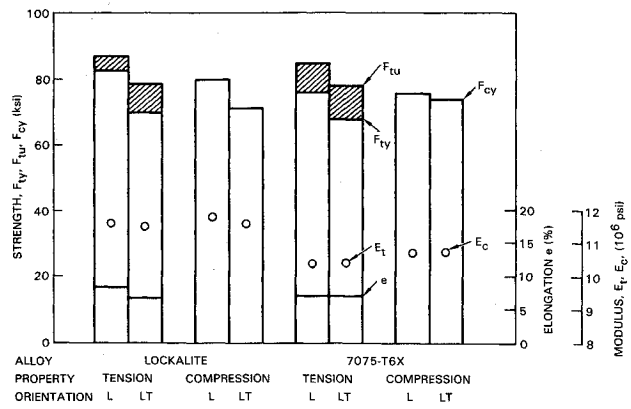

Fig. 4 Tension and compression properties for IM Al-Li alloy extrusions.

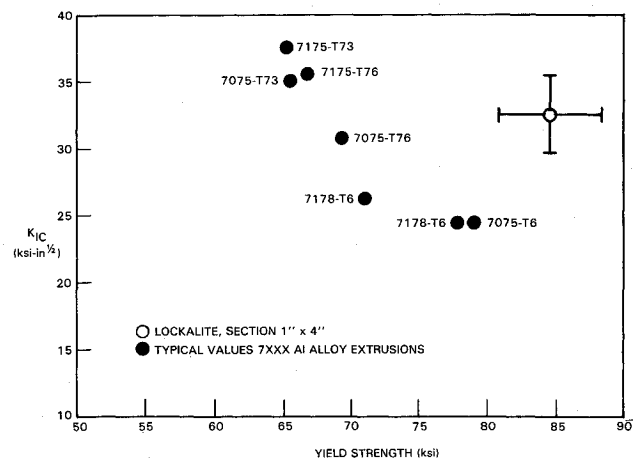

Fig. 5 Comparison of fracture toughness and strength combinations for high-strength aluminum alloy extrusions.

Structural Tests

Specimens and Test Arrangements

Two integrally stiffened compression panels approximately 18 in. long were machined from the extruded plank to the configuration shown in Fig. 6a. Identical panels, shown in Fig. 6b, were also fabricated from 7075-T73 aluminum extruded bar. The 7075-T73 extruded aluminum was selected for comparison with Al-Li, because the coupon tests indicated the compression strength of the Al-Li panels would be equal to or greater than the compressive strength of 7075-T73 panels. The panels were designed so that three equally spaced risers could

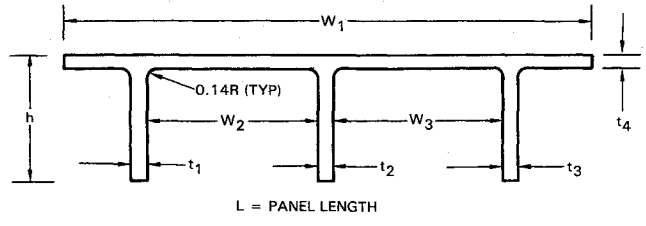

Table 4 Summary of panel dimensions

	Panel dimensions, in.								
Panel	h	t_1	t_2	t_3	t_4	W_1	W_2	W_3	L
1	1.051	0.144	0.136	0.138	0.1005	4.505	1.556	1.544	17.83
2	1.053	0.140	0.136	0.141	0.0965	4.500	1.556	1.555	17.80
3	1.052	0.138	0.136	0.132	0.0975	4.505	1.556	1.554	17.83
4	1.052	0.142	0.137	0.140	0.1040	4.504	1.556	1.554	17.81

Table 5 Section properties of test panels

Panel	Material	Section properties			
		Area, in.^{2}	$\bar{y}$, in.[a]	I in.^{4}[b]	RHO in.[c]
1	7075-T73	0.875	0.291	0.0894	0.319
2	Al-Li	0.859	0.305	0.0840	0.313
3	7075-T73	0.0853	0.290	0.8740	0.320
4	Al-Li	0.0891	0.289	0.9020	0.318

[a]Distance to neutral axis from skin side of panel.
[b]Section modulus.
[c]Radius of gyration.

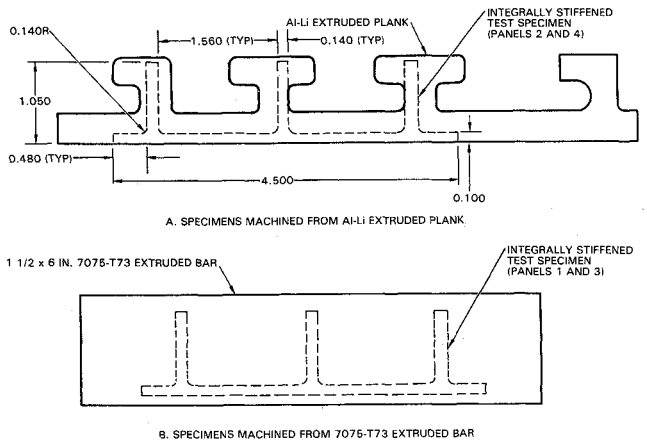

Fig. 6 Cross section of integrally stiffened compression panels machined from extrusions.

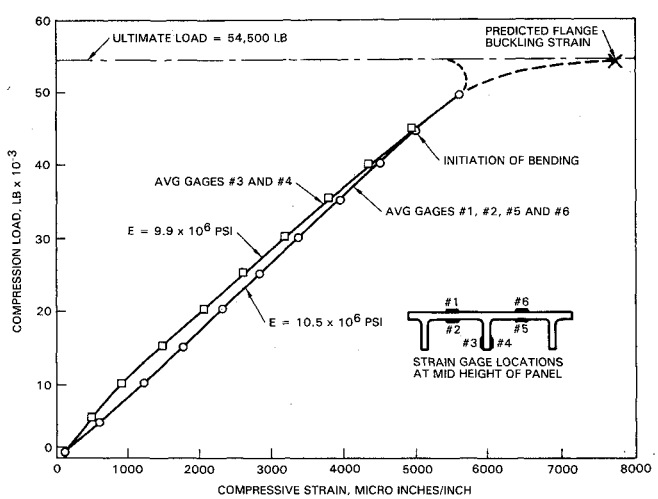

Fig. 7 Strain gage data for 7075-T73 aluminum panel 1.

be machined from the Al-Li extruded plank. The grain flow characteristics in the skin and the junction between skin and riser are similar for both extrusions, because of the selected panel locations (refer to Fig. 6). At the midheight of the risers, the grain flow is somewhat perturbed in the Al-Li panels, although a significant influence is not expected on test results.

The compression panels were sized so that column buckling would be more critical than localized buckling of the skin and risers.[12] Table 4 summarizes the results of measurements made on each panel. The final dimensions were very close to the nominal dimensions given in Fig. 6a. The ends of the panels were machined flat, square, and parallel to within ± 0.0005 in. The section properties given in Table 5 were calculated using the dimensions given in Table 4.

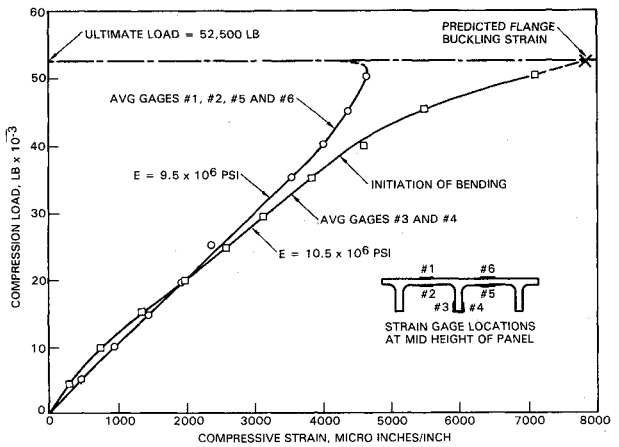

Fig. 8 Strain gage data for Al-Li panel 2.

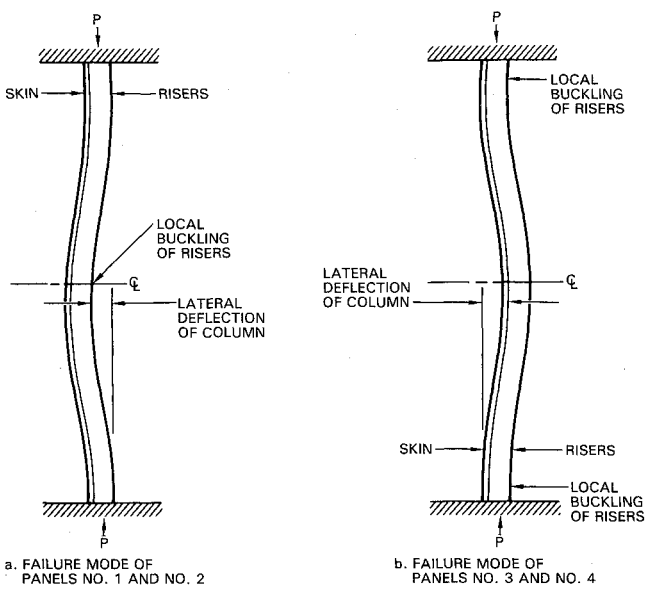

Fig. 9 Schematic of failure modes for 7075-T73 aluminum and Al-Li integrally stiffened panels.

The compression tests were conducted at California State Polytechnic University at Pomona.[13] The tests were conducted in a Tinius Olsen hydraulically actuated test machine located in the Strength of Materials Laboratory on the Pomona University Campus. The specimens were tested flat-ended between flat square plates that were surface ground to a very smooth finish. Back-to-back strain gages (Micro Measurement Type CEA-00-125UW-120) were installed at the middle of the panels at three locations: on the skin midway between the risers at two locations, and at the end of the middle riser.

Test Results

The panels were loaded incrementally to failure. Strain readings and lateral deflection measurements were recorded at each load increment. Typical results of the strain gage readings are plotted in Figs. 7 and 8. The back-to-back gages read approximately the same value of strain at all load levels. This indicates that no localized skin or flange buckling occurred up to the maximum load that was recorded for the strain readings. In all cases, the load-strain curves exhibited essentially a linear relationship up to the point indicated as "initiation of bending." When bending occurred, the skin gage readings curved in one direction, and the flange gage readings curved in the opposite direction. For panels 1 and 2, the bending increased the compressive strain in gages 3 and 4 on the riser, and decreased the compressive strain in the skin gages. For panels 3 and 4, the bending strains were in the opposite

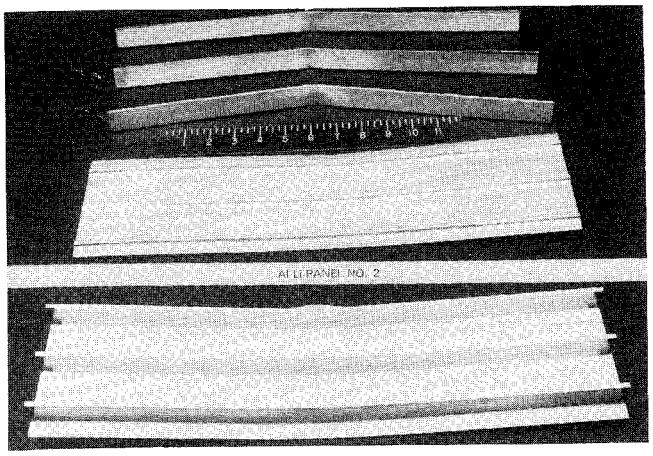

Fig. 10 Failed Al-Li and 7075-T73 panels 1 and 2.

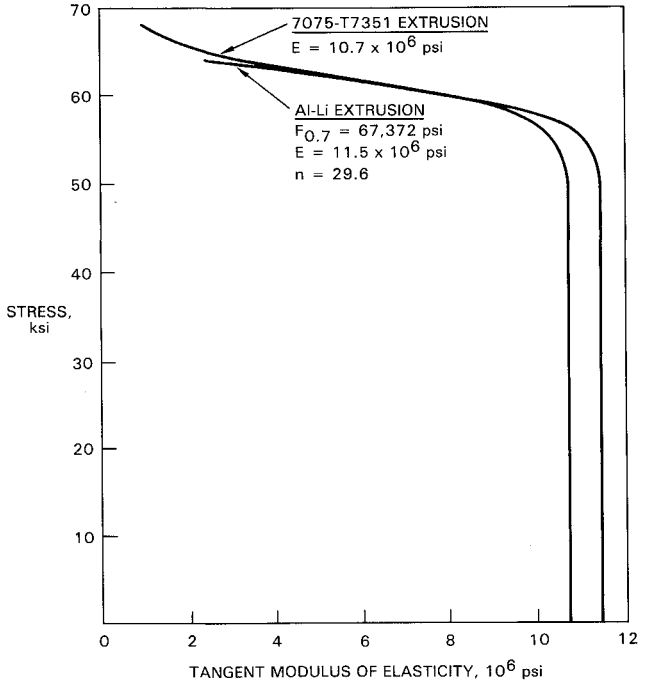

Fig. 11 Tangent modulus of elasticity for 7075-T73 aluminum and Al-Li extrusions.

direction; i.e., increasing the compressive strain in the skin gages and decreasing the compressive strain in the flange gages. This behavior is typical of compression tests conducted on columns as the compressive load approaches the failure load.[14]

The elastic stiffness of the panels, given by the initial slopes of the load-strain curves, is indicated by the values of E on Figs. 7 and 8. The stiffnesses were obtained by dividing the slope by the calculated cross-sectional area given in Table 5. If these panels were uniformly loaded with no eccentricity, the slopes of these curves would be approximately equal to the moduli of elasticity of 10.7×10^6 psi for 7075-T73 aluminum and 11.5×10^6 psi for Al-Li. It is apparent that the stiffnesses obtained from the skin gage measurements agree very well with the moduli values for these two materials. The fact that the slopes are different for the flange gages and skin gages indicates that the skin and flanges were not being loaded equally and uniformly. This difference in strain was small and within the accuracy of measurements up to the "initiation of bending" load.

The mode of failure of the four panels is depicted schematically in Fig. 9. Panels 1 and 2 failed by column buckling and

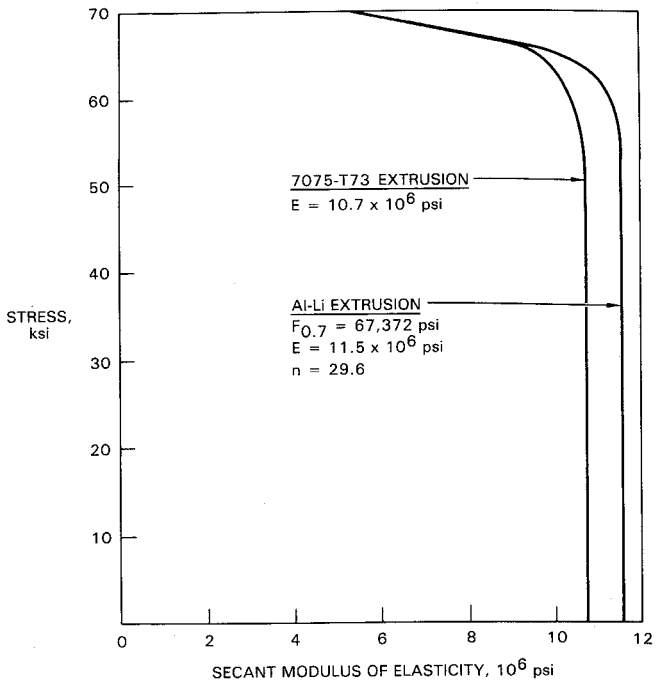

Fig. 12 Secant modulus of elasticity for 7075-T73 aluminum and Al-Li extrusions.

local buckling of the risers at the midheight of the panels, as shown in Fig. 9a. At failure of panel 2, the risers separated from the skin at the top of the fillet radius. A photo of failed panels 1 and 2 is shown in Fig. 10. Panels 3 and 4 also failed by column buckling with local flange buckling occurring at the ends of the panel as shown in Fig. 9b. The risers also separated from the skin at the top of the fillet radius on panel 4. As a result of differences in lateral deflection of the columns, the compressive strain in the flanges of panels 1 and 2 is highest at the center of the panel. Panels 3 and 4 deflected laterally in the opposite direction, producing the highest compressive strain in the risers at the ends of the panels. Separation of the risers from panels 2 and 4 is attributed to the lower ductility of Al-LI alloys in the short-transverse (ST) grain direction across the riser thickness compared to 7075-T73 aluminum. The elongation of some Al-Li alloys is reported to be less than 2% in the ST direction. High tensile strains are induced at the base of the flanges when the flanges buckled at panel failure.

Comparison of Predictions and Test Results

The preliminary analysis using a Lockheed-Advanced Structures computer program indicated that the panels would fail in column buckling. The predicted local buckling stress of the cross section was much higher than the predicted column buckling strength. In the computerized analysis, the predicted stability loads cannot be exceeded unless localized buckling occurs at stresses below the predicted stability loads. Based on the results of this analysis and the following discussions, column buckling is considered the primary mode of failure, and localized buckllling of the flanges the secondary mode of failure.

The column buckling strength was predicted using the tangent modulus formula given by:[14]

$$F_{cr} = \frac{\pi^2 E_t}{(L_e/l)^2} \tag{1}$$

The tangent modulus of elasticity as a function of the applied stress is given in Fig. 11 for the two materials. The tangent modulus for Al-Li alloy material was calculated based on values of $F_{0.7}$ and n obtained from tension stress-strain curves. The end fixity coefficient of $c = 3.5$ was based on experience obtained on other compression panels tested in a flat-ended

Table 6 Summary of test results and predictions for compression panel tests

Panel	Material	Initiation of bending		Panel failure		Predicted failure
		Load, lb	Stress, psi	Load, lb	Stress, psi	Stress, psi[a]
1	7075-T73	45,000	51,429	54,500	62,286	62,000
2	Al-Li	37,500	43,655	52,500	61,118	61,500
3	7075-T73	43,500	50,996	54,450	63,834	62,000
4	Al-Li	43,500	48,822	56,500	63,412	61,500

[a]Column buckling using tangent modulus of elasticity.

configuration. The radius of gyration of each panel cross section is given in Table 5.

The comparison between predicted column strength and test results is given in Table 6. The predicted failure stress is very close to the ultimate stress at failure of each panel. Also, the predicted failure stress and the panel failure stress are approximately the same for the two 7075-T73 aluminum panels and the two Al-Li panels. This is because the tangent modulus of elasticity for the two materials is approximately the same for stress levels above 58,000 psi, as shown in Fig. 11. Therefore, the column strength is equivalent for panels designed from the two materials for stress levels above 58,000 psi. However, the Al-Li panels would be approximately 8% lighter because of the differences in density between the two materials. For stress levels below 58,000 psi, the Al-Li panel would save additional weight because the modulus of elasticity is higher, as shown in Fig. 11. Weight saving analysis[15] indicates a 13% weight saving potential for a compression surface column mode of failure.

As shown in Fig. 8, the compressive strain in the flanges at the center of the column increases asymptotically to the failure load, while the strain in the skin decreases near panel failure. The compressive strain in the flanges is highest at the center of the column for panels 1 and 2 because of the lateral bending of the column as depicted in Fig. 9a. Therefore, localized buckling of the flanges at the center of the column is expected to occur at the failure load as the compressive strain approaches the critical value. For panels 3 and 4 the highest compressive strain in the flanges occurs at both ends of the column as depicted in Fig. 9b, and localized flange buckling would be expected to occur there. Where localized buckling occurred in the flanges, the compressive strain was much lower in the skin.

To predict localized buckling of the flanges, it is assumed that the flanges were simply supported by the skin. This occurs because the local strains in the skin at the locations of flange buckling were decreasing as the applied load approached the failure load, while the local strains in the flanges were increasing. The buckling stress of long flanges simply supported on one edge can be predicted from the following equation:[13]

$$F_{cr} = k_c E_s (t/b)^2 \qquad (2)$$

For a long flange with one edge free and one edge simply supported, k_c is equal to 0.375. The secant moduli of elasticity for the two materials are plotted in Fig. 12. The width b of the flange was measured from the riser side of the skin.

The flange buckling stress for the panels was calculated to be 66,300 psi for panels 1 and 3, and 66,800 psi for panels 2 and 4. These stress values correspond to compressive strain levels of 7600 and 7800 μin./in. for 7075-T73 aluminum and Al-Li panels, respectively. By extrapolation of the curves in Figs. 7 and 8, these critical strain levels in the flanges are achieved at loads very close to the ultimate load. The flanges of panels 3 and 4 buckled at the ends of the panels where no strains were recorded, but it is assumed the same type of behavior occurred in these two panels.

Based on the data obtained during testing and the subsequent analyses, the failure sequence of the panels can be described as follows. As compression load is applied to the specimens, the compression strain increases linearly until the column starts to bend. For these panels, this occurred at approximately the proportional limit stress of the material as indicated in Table 6. As the load is increased further, the bending strains increase more on one side of the panel than on the other side. Near the tangent modulus predicted failure load for column buckling, the compressive strains in the flanges have increased sufficiently to cause flange buckling. When flange buckling occurs, the stiffness of the column is further reduced, and complete failure ensues. Whether flange buckling occurs at the center of the column or at the ends of the column is related to the direction of column bending, as indicated in Fig. 9. If the ductility of the material is low, as for Al-Li alloys in the ST orientation, the risers can separate from the skin when flange buckling occurs. Even if flange buckling did not occur, these panels could not support significantly higher compression loads, because the tangent and secant moduli of elasticity for both materials decreases rapidly for higher stresses as shown in Figs. 11 and 12.

Conclusions

A materials characterization and structural behavior study on Al-Li alloy extrusions has been described in the preceding sections. The experimental results and analyses have led to the following conclusions:

1) The mechanical property behavior of the candidate Al-Li alloy, designated LOCKALITE, represents a suitable replacement for conventional 7075-T76X and 7075-T73X aluminum extrusions.

2) The results of stiffened compression panel tests using both Al-Li and 7075 aluminum alloys are consistent with prediction methods involving stress analyses and material properties.

3) The application of Al-Li alloys in compression critical structures contributes to a weight savings of 8% due to density reduction, and an overall savings of up to 13% based on specific modulus improvements.

Acknowledgments

The authors wish to express their appreciation to the following people who contributed to the results presented in this paper: D. G. Richardson for designing the test panels; R. E. Wood for the fabrication of the test panels; R. A. Rainen and T. Gillette for performing the Al-Li material property evaluations; and D. A. Afarian, a senior student at California State Polytechnic University, for conducting the compression tests of the stiffened panels.

References

[1]Grimes, R., Miller, W. S., Reynolds, M. A., and Gray, A., "Aluminum-Lithium: The Successes and the Problems," presented at Western Metal and Tool Exposition and Conference, Los Angeles, CA, March 1986.

[2]Bretz, P. E., "Low Density Aluminum-Technology," presented at Western Metal and Tool Exposition and Conference, Los Angeles, CA, March 1986.

[3]LeRoy, G. and Meyer, P., "Status Report on the Development of Aluminum-Lithium at Pechiney," presented at Western Metal and Tool Exposition and Conference, Los Angeles, CA, March 1986.

[4]Lewis, R. E., Webster, D., and Palmer, I. G., "A Feasibility Study for Development of Structural Aluminum Alloys from Rapidly Solidified Powders for Aerospace Structural Applications," Interim Tech., AFML TR-78-102, July 1978.

[5]Narayan, G. H., Quist, W. E., Wilson, B. L., and Wingert A. L., "Low Density Aluminum Alloy Development," First Interim Tech. Rept., AFML Contract F33615-81-C-5051, Rept. D6-51411, August 1982.

[6]Langenbeck, S. L., Sakata, I. F., and Sawtell, R. R., "Aerospace Structural Application of Aluminum-Lithium," presented at Western Metal and Tool Exposition and Conference, Los Angeles, CA, March 1986.

[7]Chellman, D. J., Rainen, R. A., Divecha, A. P., and Garrett, R. K., Jr., "Influence of Solute Content on Properties of IM Al-Li-Cu-Mg-(Zr) Alloys," presented at Western Metal and Tool Exposition and Conference, Los Angeles, CA, March 1984.

[8]Ekvall, J. C. and Chellman, D. J., "Ingot Metallurgy Aluminum-Lithium Alloys for Aircraft Structure," *Journal of Aircraft*, Vol. 24, April 1987, pp. 255–261.

[9]Chellman, D. J. and Rainen, R. A., "Influence of Composition and Processing Variables on Property Behavior of an IM Al-Li-Cu-Mg-(Zr) Alloy (LOCKALITE)," Third International Aluminum-Lithium Conference, Oxford, England, July 1985.

[10]Chellman, D. J., Rainen, R. A., Divecha, A. P., and Garrett, R. K., Jr., "Property and Microstructure Characterizations for the Novel IM Al-Li-Mg-Cu-(Zr) Alloy System," The 115th Metal Society–American Institute of Mechanical Engineers Meeting, New Orleans, LA, March 1985.

[11]*Metallic Materials and Elements for Aerospace Vehicle Structures*, Military Standardization Handbook MII-HDBK-5E, June 1987.

[12]Contini, R., "Margins of Safety for Unflanged Integrally Stiffened Sheet Wing Surfaces," Lockheed Aeronautical Systems Company Rept. 22808, Rev. A, Oct. 15, 1985.

[13]Afarian, D. A., "Compression Failure Load Determination, California State Polytechnic University Pomona Senior Project ETT 461, 462, Summer 1985," Pomona, CA, Aug. 1985.

[14]Shanley, F. R., *Strength of Materials*, McGraw-Hill, New York, NY, 1957, pp. 582, 612–613.

[15]Ekvall, J. C., "Summary Report of 1983–84 Independent Research on Advanced Metallic Structures," Lockheed Aeronautical Systems Company Rept. 30834, Dec. 1984.